SHISA6 Confers Resistance to Differentiation-Promoting Wnt/β-Catenin Signaling in Mouse Spermatogenic Stem Cells

AUTHOR(S):

Tokue, Moe; Ikami, Kanako; Mizuno, Seiya; Takagi, Chiyo; Miyagi, Asuka; Takada, Ritsuko; Noda, Chiyo; ... Takahashi, Satoru; Takada, Shinji; Yoshida, Shosei

CITATION:

Tokue, Moe ...[et al]. SHISA6 Confers Resistance to Differentiation-Promoting Wnt/β-Catenin Signaling in Mouse Spermatogenic Stem Cells. Stem Cell Reports 2017, 8

ISSUE DATE:

2017-02-09

URL:

http://hdl.handle.net/2433/218789

Please cite this article in press as: Tokue et al., SHISA6 Confers Resistance to Differentiation-Promoting Wnt/β-Catenin Signaling in Mouse Spermatogenic Stem Cells, Stem Cell Reports (2017), http://dx.doi.org/10.1016/j.stemcr.2017.01.006

Stem Cell Reports
Article
ISSCR
OPEN ACCESS

SHISA6 Confers Resistance to Differentiation-Promoting Wnt/β-Catenin Signaling in Mouse Spermatogenic Stem Cells

Moe Tokue,[1,2] Kanako Ikami,[1,2,13] Seiya Mizuno,[3] Chiyo Takagi,[4] Asuka Miyagi,[4,14] Ritsuko Takada,[5,6] Chiyo Noda,[7] Yu Kitadate,[1,2] Kenshiro Hara,[1,2,8] Hiroko Mizuguchi,[1] Takuya Sato,[9] Makoto Mark Taketo,[10] Fumihiro Sugiyama,[3] Takehiko Ogawa,[9] Satoru Kobayashi,[2,6,7,11] Naoto Ueno,[2,4] Satoru Takahashi,[3,12] Shinji Takada,[2,5,6] and Shosei Yoshida[1,2,*]

[1]Division of Germ Cell Biology, National Institute for Basic Biology, National Institutes of Natural Sciences, Okazaki 444-8787, Japan
[2]Department of Basic Biology, School of Life Science, Graduate University for Advanced Studies (Sokendai), Okazaki 444-8585, Japan
[3]Laborarory Animal Resource Center, University of Tsukuba, Tsukuba 305-8575, Japan
[4]Division of Morphogenesis, National Institute for Basic Biology, National Institutes of Natural Sciences, Okazaki 444-8585, Japan
[5]Division of Molecular and Developmental Biology, National Institute for Basic Biology, National Institutes of Natural Sciences, Okazaki 444-8787, Japan
[6]Okazaki Institute for Integrative Bioscience, National Institutes of Natural Sciences, Okazaki 444-8787, Japan
[7]Division of Developmental Genetics, National Institute for Basic Biology, National Institutes of Natural Sciences, Okazaki 444-8787, Japan
[8]Laboratory of Animal Reproduction and Development, Graduate School of Agricultural Science, Tohoku University, Sendai 981-8555, Japan
[9]Laboratory of Proteomics, Institute of Molecular Medicine and Life Science, Yokohama City University Association of Medical Science, Yokohama 236-0004, Japan
[10]Division of Experimental Therapeutics Graduate School of Medicine, Kyoto University, Kyoto 606-8501, Japan
[11]Life Science Center of Tsukuba Advanced Research Alliance, University of Tsukuba, Tsukuba 305-8577, Japan
[12]Department of Anatomy and Embryology, Faculty of Medicine, University of Tsukuba, Tsukuba 305-8575, Japan
[13]Present address: Department of Cell and Developmental Biology, University of Michigan Medical School, Ann Arbor, MI 48109, USA
[14]Present address: Core Biotechnology Services, Advanced Research Facilities and Services, Preeminent Medical Photonics Education and Research Center, Hamamatsu University School of Medicine, Hamamatsu 431-3192, Japan
*Correspondence: shosei@nibb.ac.jp
http://dx.doi.org/10.1016/j.stemcr.2017.01.006

SUMMARY

In the seminiferous tubules of mouse testes, a population of glial cell line-derived neurotrophic factor family receptor alpha 1 (GFRα1)-positive spermatogonia harbors the stem cell functionality and supports continual spermatogenesis, likely independent of asymmetric division or definitive niche control. Here, we show that activation of Wnt/β-catenin signaling promotes spermatogonial differentiation and reduces the GFRα1$^+$ cell pool. We further discovered that SHISA6 is a cell-autonomous Wnt inhibitor that is expressed in a restricted subset of GFRα1$^+$ cells and confers resistance to the Wnt/β-catenin signaling. *Shisa6*$^+$ cells appear to show stem cell-related characteristics, conjectured from the morphology and long-term fates of *T* (*Brachyury*)$^+$ cells that are found largely overlapped with *Shisa6*$^+$ cells. This study proposes a generic mechanism of stem cell regulation in a facultative (or open) niche environment, with which different levels of a cell-autonomous inhibitor (SHISA6, in this case) generates heterogeneous resistance to widely distributed differentiation-promoting extracellular signaling, such as WNTs.

INTRODUCTION

Stem cells support tissue homeostasis through continual production of differentiating progeny based on the maintenance of an undifferentiated cell pool. This is traditionally thought to depend on a couple of paradigmatic mechanisms: asymmetric cell division, which always gives rise to one self-renewing cell and one differentiating cell; and the control by an anatomically defined niche, inside which stem cells remain undifferentiated, but differentiate when they move out (Fuller and Spradling, 2007; Morrison and Spradling, 2008). These mechanisms coexist in some tissues, such as the *Drosophila* female and male germlines (Spradling et al., 2011), while niche regulation may not accompany asymmetric cell division, as observed in the mouse intestinal crypt (Snippert et al., 2010).

Mouse spermatogenesis represents actively cycling stem cell-supported tissue, which occurs in the testicular seminiferous tubules (Figure 1A). Here, all spermatogonia (mitotic germ cells) are located in the basal compartment, i.e., the gap between the basement membrane and the tight junction among Sertoli cells (Russell et al., 1990). Germ cells then translocate to the adluminal compartment, undergo meiotic divisions, and differentiate into haploid spermatids. Spermatogonia are largely divided into "undifferentiated" and "differentiating" spermatogonia (Figure 1B) (de Rooij and Russell, 2000; Yoshida, 2012). In the steady state, the stem cell function resides in the glial cell-derived neurotrophic factor (GDNF) family receptor alpha 1 (GFRα1)-positive (+) subset of undifferentiated spermatogonia. GFRα1$^+$ cells maintain their population and differentiate neurogenin 3 (NGN3)$^+$ subset of undifferentiated spermatogonia (Hara et al., 2014; Nakagawa et al., 2010). NGN3$^+$ cells express retinoic acid (RA) receptor gamma (RARγ) and, in response to the RA pulse which occurs once every 8.6-day cycle of seminiferous epithelium, differentiate into differentiating spermatogonia (KIT$^+$) that experience a series of mitotic divisions

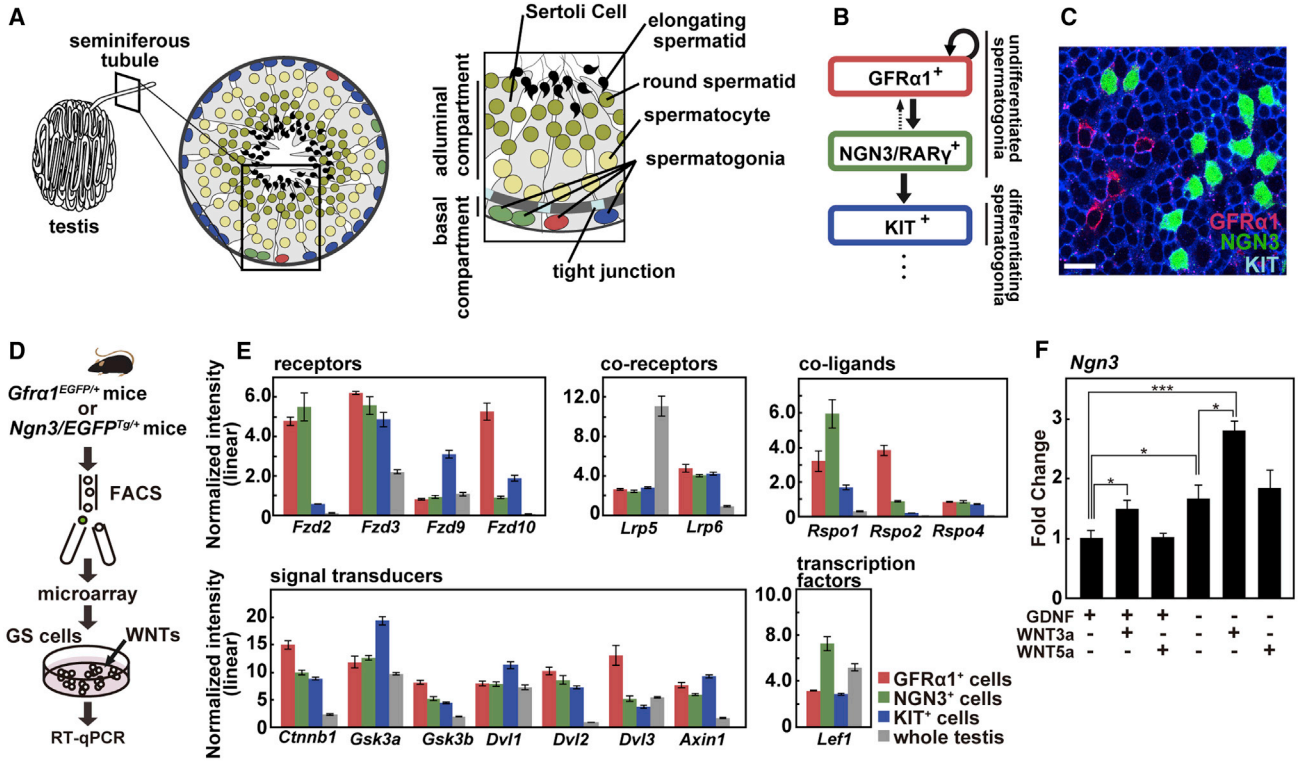

Figure 1. Identification of Wnt/β-Catenin Signaling as an Inducer of Spermatogonial Differentiation

(A and B) Schematics of testis structure (A) and the functional relationship between GFRα1$^+$, NGN3$^+$, and KIT$^+$ cells (B). See text for details.

(C) A triple-staining image of the basal compartment showing the intermingling of GFRα1$^+$, NGN3$^+$, and KIT$^+$ cells. Scale bar, 20 μm.

(D) Experimental sequence for screening of cells' extrinsic factors.

(E) Expression of Wnt/β-catenin pathway-related genes indicated in GFRα1$^+$, NGN3$^+$, and KIT$^+$ fractions and whole testes, summarized from the microarray data. Represented as means ± SEM (n = 3 microarrays, each form different mice).

(F) Expression of *Ngn3* mRNA in GS cells in the presence or absence of GDNF, WNT3a, or WNT5a. GS cells cultured on laminin-coated plates for 24 hr were switched to the indicated conditions and cultured for an additional 24 hr, followed by quantitative real-time PCR analysis of *Ngn3* mRNA. Represented as means ± SEM (n = 3 independent experiments). *p < 0.05, ***p < 0.001 (Student's t test). See also Figure S1.

before meiosis (Gely-Pernot et al., 2012; Hogarth et al., 2015; Ikami et al., 2015; Sugimoto et al., 2012). NGN3$^+$ cells, however, remain capable of reverting to GFRα1$^+$ cells and self-renewing, which becomes prominent in regeneration after damage or transplantation (Nakagawa et al., 2007, 2010). The GFRα1$^+$ population is comprised of singly isolated cells (called A_s) and syncytia of two or more cells (A_{pr} or A_{al}, respectively); It is under current discussion whether the steady-state stem cell function is restricted to its subsets (e.g., fractions of A_s cells), or extended over the entirety of GFRα1$^+$ cells (Yoshida, 2017).

Interestingly, this stem cell system appears not to rely on asymmetric division or definitive niche regulation. The fate of pulse-labeled GFRα1$^+$ cells shows dynamics of "population asymmetry," in which individual cells follow variable and stochastic fates rather than the stereotypic pattern of "division asymmetry" (Hara et al., 2014; Klein et al., 2010; Klein and Simons, 2011). Definitive niche control is also unlikely, because GFRα1$^+$ cells are not clustered to particular regions, but scattered between NGN3$^+$ and KIT$^+$ cells (Figure 1C) (Grasso et al., 2012; Ikami et al., 2015), with some biases to the vasculature and interstitium (Chiarini-Garcia et al., 2001, 2003; Hara et al., 2014). Furthermore, GFRα1$^+$ cells have been filmed intravitally to continually migrate between immotile Sertoli cells (Hara et al., 2014; Yoshida et al., 2007). Such a non-canonical stem cell environment is known as a "facultative (open) niche," contrary to the classical "definitive (closed) niche" (Morrison and Spradling, 2008; Stine and Matunis, 2013). It is an open question as to how the heterogeneous stem cell fates (to differentiate and to remain undifferentiated) cohabit in facultative niche environments.

To regulate the GFRα1$^+$ cell pool, GDNF plays a key role. GDNF is expressed in Sertoli and myoid cells, and acts on GFRα1$^+$ cells through the receptor composed of GFRα1 and RET (Airaksinen and Saarma, 2002). GDNF inhibits

Please cite this article in press as: Tokue et al., SHISA6 Confers Resistance to Differentiation-Promoting Wnt/β-Catenin Signaling in Mouse Spermatogenic Stem Cells, Stem Cell Reports (2017), http://dx.doi.org/10.1016/j.stemcr.2017.01.006

the differentiation of GFRα1$^+$ spermatogonia cultured in vitro (Kanatsu-Shinohara et al., 2003; Kubota et al., 2004). Consistently, impaired GDNF signaling in vivo caused by loss-of-function mutations in *Gdnf*, *Gfra1*, and *Ret* reduces the GFRα1$^+$ cell pool through enhanced differentiation (Jijiwa et al., 2008; Meng et al., 2000; Sada et al., 2012). Fibroblast growth factor (FGF) signaling also inhibits the differentiation of GFRα1$^+$ cells in vitro, supported by relatively limited in vivo evidence (Hasegawa and Saga, 2014; Kubota et al., 2004). However, mechanisms that promote the differentiation of GFRα1$^+$ cells and that underline their heterogeneous fates remain largely unknown.

Wnt signaling has pleiotropic functions including stem cell regulation. In many cases, the "canonical" Wnt pathway, mediated by β-catenin, acts to maintain the stem cell pool by inhibiting their differentiation (Clevers and Nusse, 2012). In mouse spermatogenesis, however, studies using cultured spermatogonia suggest that Wnt/β-catenin signaling (activated by WNT3a) stimulates the proliferation of differentiating progenitors (Yeh et al., 2011, 2012). Similarly, in vivo, Wnt/β-catenin signal is implicated for the generation and/or proliferation of differentiating progenitors, because *β-catenin* deletion reduced the total number of undifferentiated spermatogonia (PLZF$^+$), while the GFRα1$^+$ pool was unaffected (Takase and Nusse, 2016). Nevertheless, the precise roles of Wnt/β-catenin signaling in the GFRα1$^+$ pool remain elusive, due to the lack of markers and the nature of the genetic tools.

In this study, by searching for differentiation-promoting factor(s), we found that Wnt/β-catenin signaling drove the GFRα1$^+$ to NGN3$^+$ differentiation. Further, we discovered that SHISA6 is a cell-intrinsic Wnt inhibitor with restricted expression to a subset of GFRα1$^+$ cells. In vitro and in vivo analyses illustrate the key roles of *Shisa6* and SHISA6$^+$ cells in this stem cell system.

RESULTS

Wnt/β-Catenin Signaling Promotes Spermatogonial Differentiation

To elucidate cell-extrinsic signals promoting the differentiation of GFRα1$^+$ cells, we first examined the transcriptomes of GFRα1$^+$ and NGN3$^+$ spermatogonia (Figure 1D). GFRα1$^+$ and NGN3$^+$ fractions were collected from adult *Gfra1*$^{EGFP/+}$ (Enomoto et al., 2000) and *Ngn3/EGFP*$^{Tg/+}$ mice (Yoshida et al., 2004), respectively, by fluorescence-activated cell sorting (Figure S1A). Subsequent cDNA microarray analysis revealed the signaling pathways that potentially act in these cells (Figure S1B).

In particular, the Wnt/β-catenin signaling components, including receptors/co-receptors, signal transducers/modulators, and transcription factors were found to be expressed GFRα1$^+$ and NGN3$^+$ cells (Figures 1E and S1C). *Lef1*, a transcription factor gene, is also a downstream target of this pathway (Hovanes et al., 2001). These data indicate that both GFRα1$^+$ and NGN3$^+$ cells receive Wnt/β-catenin signals, consistent with a previous study using *Axin2* reporters (Takase and Nusse, 2016). The higher level of *Lef1* expression suggests that NGN3$^+$ cells may receive a stronger signal than GFRα1$^+$ cells.

Next, we tested the effect of Wnt/β-catenin signaling in vitro using germline stem (GS) cells: GDNF-dependent cultures of spermatogonia retaining GFRα1 expression and stem cell activity (Kanatsu-Shinohara et al., 2003). We found that the addition of WNT3a (an activator of the β-catenin pathway), but not WNT5a (an activator of β-catenin-independent pathway), increased the *Ngn3* mRNA in the presence or absence of GDNF (Figure 1F).

Elevated Wnt/β-Catenin Signaling Reduces the GFRα1$^+$ Cell Pool In Vivo

We then asked what the in vivo role of Wnt/β-catenin signaling is, using *β-catenin* mutants. To strengthen the signal by stabilizing β-catenin protein, we used the *Ctnnb1*$^{fl(ex3)}$ allele, which enables the conditional deletion of exon 3 encoding critical GSK3β phosphorylation sites (Figure 2A) (Harada et al., 1999). To reduce the signal, a conditionally null, *Ctnnb1*^{fl}, allele was used (Figure S3A) (Brault et al., 2001). These mutations were specifically and efficiently induced into germ cells using the *Nanos3*^{Cre} allele (Figures S2A and S2B) (Suzuki et al., 2008). Since the following analyses were performed in the *Nanos3*$^{Cre/+}$ background, the genotypes will be simply indicated by the *β-catenin* alleles.

Although the impact of the stabilized β-catenin was not apparent in the heterozygotes [*fl(ex3)/+*], it was obvious in the homozygotes [*fl(ex3)/fl(ex3)*]. At 8–14 weeks of age, *fl(ex3)/fl(ex3)* mice showed smaller testes, with body weight unchanged (Figures 2B–2F). Their testes showed spermatogenesis defects (e.g., loss or exiguousness of one or more germ cell layers) in about 20% of the tubule sections (Figures 2G–2J). Notably, the number of GFRα1$^+$ cells was reduced in the homozygotes (Figures 2K and S2C–S2E), without significant reduction of RARγ$^+$ cells (largely corresponding to NGN3$^+$ cells) (Gely-Pernot et al., 2012; Ikami et al., 2015), resulting in the increased RARγ$^+$ cell-to-GFRα1$^+$ cell ratio (Figures 2L, 2M, and S2C–S2E). *fl(ex3)/fl(ex3)* mice showed normal testicular morphology and GFRα1$^+$ cell numbers at post-natal day 3 (P3), indicating the normal fetal and neonatal germ cell development (Figures S2F–S2I). To summarize, the elevated Wnt/β-catenin signal reduced the GFRα1$^+$ cell pool in a dose-dependent manner.

Deletion of *β-catenin* caused largely consistent phenotypes (Figures S3B–S3J). Although the number of GFRα1$^+$

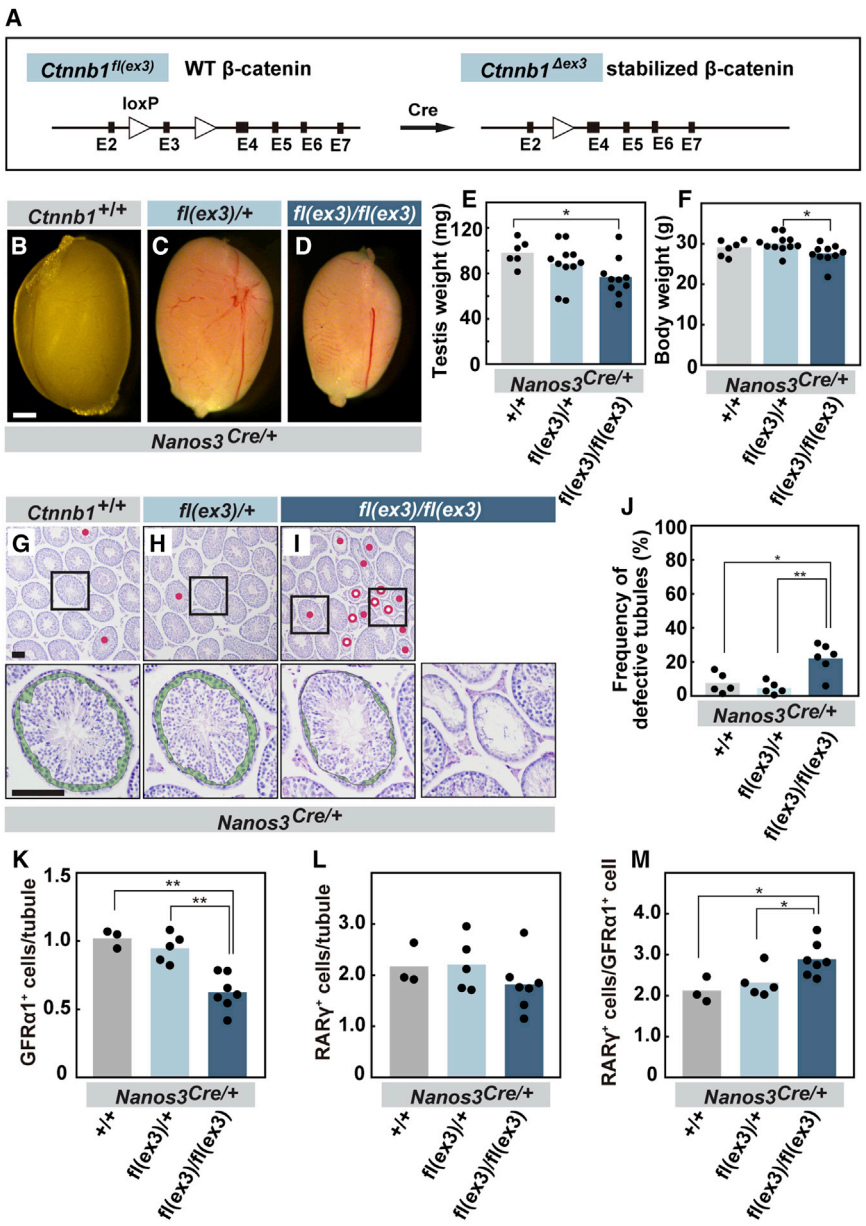

Figure 2. Impact of Stabilized β-Catenin on Spermatogenesis In Vivo

(A) Schematics of the *Ctnnb1*$^{fl(ex3)}$ allele, producing stabilized β-catenin protein after Cre-mediated recombination.

(B–F) Representative appearance of the adult mice testes for the indicated genotypes (B–D), and their testis weights (E) and body weights (F). Scale bar, 1 mm.

(G–I) Histological images of testicular sections of adult mice for the indicated genotypes, stained with PAS-hematoxylin. Lower panels are the magnified images of the indicated regions in the upper panels. Open and closed red dots indicate the tubule sections with lost or exiguous germ cell layer(s) (see the lower panels, showing tubule sections at stage II-III in which pachytene spermatocytes layer is colored green), and those containing Sertoli cells only; see the lower right panel of (I), respectively. Scale bar, 100 μm.

(J) Percentages of the total defective tubules (lost or exiguous germ cell layer(s)) with indicated genotypes.

(K–M) Average numbers of GFRα1$^+$ (K) and RARγ$^+$ (L) cells per tubule, and the ratio between RARγ$^+$ cells and GFRα1$^+$ cell (M), for the indicated genotypes, based on double IF for GFRα1 and RARγ on testicular sections (as shown in Figures S2C–S2E). Only the cells located in tubule sections showing orbicular shape were counted. Throughout, mice were analyzed at the age of 8–14 weeks, and the actual values from different individuals and their averages are shown by dots and columns, respectively.

*$p < 0.05$, **$p < 0.01$ (Student's t test). See also Figures S2 and S3.

cells did not change, the RARγ$^+$ cell number and the RARγ$^+$ cell-to-GFRα1$^+$ cell ratio decreased, consistent with the idea that GFRα1$^+$ to NGN3$^+$ differentiation was affected (Figures S3K–S3O). This was largely in agreement with the previous study (Takase and Nusse, 2016).

Seminiferous Epithelial Cycle-Related *Wnt6* Expression

By screening the expression of all mouse *Wnt* genes by in situ hybridization (ISH), we found prominent expression of *Wnt6* in Sertoli and interstitial cells (Figures 3A–3C), in agreement with a previous report (Takase and Nusse, 2016). Further, *Wnt6* expression showed a seminiferous epithelial cycle-related expression, highest in stages I to VI (Figure 3G). Of note, the increase in *Wnt6* expression coincides with the decrease in *Gdnf* (visualized by a *Gdnf-LacZ* knockin allele; Figures 3D–3G) (Moore et al., 1996), the increase in NGN3$^+$ cells, and the weak decrease in GFRα1$^+$ cells (Figure 3H). These observations largely supported the notion that the increase in *Wnt6* and the decrease in GDNF drive the GFRα1$^+$ cells to differentiate to NGN3$^+$.

However, the spatially uniform expression of these factors over a tubule cross-section raises a question: why do some GFRα1$^+$ cells differentiate into NGN3$^+$ cells, while the others remain GFRα1$^+$ in an apparently uniform

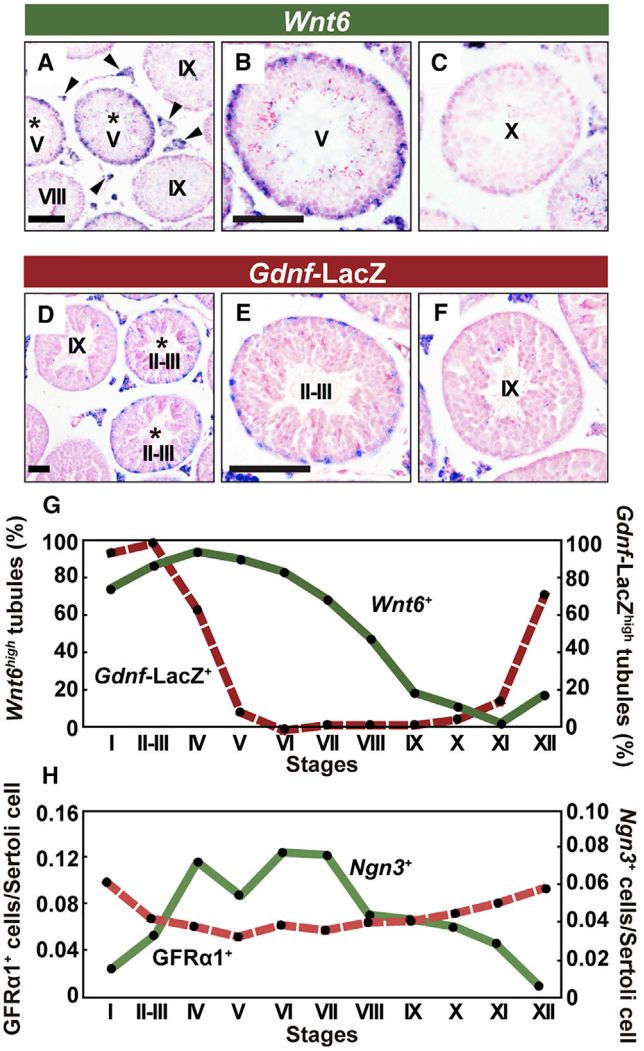

Figure 3. Seminiferous Epithelial Cycle-Related expression of *Wnt6*, *Gdnf-LacZ*, GFRα1, and *Ngn3*

(A–F) Images of adult mouse testis sections after visualizing the expression of *Wnt6* by ISH (A–C) and *Gdnf-LacZ* by β-galactosidase staining using $Gdnf^{LacZ/+}$ mice (D–F). Asterisks indicate tubules with high expression of *Wnt6* or LacZ in Sertoli cells. High-power images of *Wnt6*-or LacZ-high (B) and (E) and low/negative (C) and (F) tubules are also shown. Roman numerals indicate the stage of seminiferous tubules determined by PAS-stained adjacent sections. The expression of *Wnt6* was also detected in interstitial cells, arrowheads in (A), while that of *Gdnf-LacZ* was undeterminable due to background β-galactosidase activity. Scale bars, 100 μm.

(G) Percentage of $Wnt6^{high}$ and *Gdnf*-$LacZ^{high}$ tubules in each stage, in which Sertoli cells expressed *Wnt6* or LacZ in a major part of the tubule circumference.

(H) Numbers of GFRα1$^+$ and *Ngn3*$^+$ cells per Sertoli cell at the indicated stages, as obtained from IF- and ISH-stained testis sections, respectively. The latter was reproduced from a previous report (Ikami et al., 2015). A total of 18–144 tubule sections were counted from 2 to 5 testes, for each cell type.

environment? However, it is unlikely due to the spatial unevenness in Wnt activity generated by extracellular Wnt inhibitors because GFRα1$^+$ cells are motile and extensively interspersed between NGN3$^+$ cells (which likely receive higher Wnt signals; Figures 1C and 1E) (Hara et al., 2014; Ikami et al., 2015). We hypothesized that GFRα1$^+$ cells show different levels of cell-intrinsic resistance to Wnt/β-catenin signaling.

SHISA6 Is a Cell-Intrinsic Wnt Inhibitor Expressed in a Subset of GFRα1$^+$ Cells

We therefore searched for factor(s) that could cell-autonomously inhibit Wnt/β-catenin signaling in GFRα1$^+$ spermatogonia, among genes showing restricted expressions in the GFRα1$^+$ fraction (Figures 4A and 4B). Although known Wnt inhibitors were not highly enriched, we focused on *Shisa6*, the fourth most highly enriched gene. In testis sections, immunofluorescence (IF) detected SHISA6 protein in a few spermatogonia on the periphery of the seminiferous tubules, many of which were also GFRα1$^+$ (Figure 4C). Unfortunately, the staining condition required for SHISA6 IF was not optimal for GFRα1, so only a fraction of GFRα1$^+$ cells were detected in the double IF. We, therefore, combined fluorescence ISH for *Shisa6* with IF for GFRα1 on dispersed testicular cells, and found that a high level of *Shisa6* expression was restricted to ~30% of GFRα1$^+$ cells (Figures 4D and 4E).

We hypothesized that SHISA6 could be a cell-autonomous Wnt inhibitor, because some *Shisa* family proteins (e.g., *xshisa1*, *2*, *3*, and *mShisa2* and *3*) inhibit Wnt signaling in a cell-autonomous fashion by suppression the maturation and cell surface expression of Wnt receptors (Chen et al., 2014; Furushima et al., 2007; Nagano et al., 2006; Yamamoto et al., 2005). However, the molecular functions of SHISA6 are relatively unclear; a recent report showed that SHISA6 stabilized the AMPA receptor expression in the mouse brain, similar to SHISA9 (Klaassen et al., 2016; von Engelhardt et al., 2010).

Using *Xenopus laevis* embryos, we found that co-injection of *mShisa6* mRNA inhibited the secondary axis formation by *xwnt8* (Figures 5A–5E), as observed previously for *mShisa2* (Yamamoto et al., 2005). *mShisa6* injection alone enlarged the cement gland (Figures S4A–S4E), an indication of Wnt inhibition also observed for *xshisa1*, *xshisa2*, and *mShisa2* (Furushima et al., 2007; Yamamoto et al., 2005). Further, in HEK293T cells, *mShisa6* inhibited the activation of *TCF-luc*, a Wnt/β-catenin signaling reporter (Figure 5F) (Shimizu et al., 2012). This inhibition was observed when *Shisa6* and the reporter were co-transfected, but not when these components were transfected into separate cells and the transfected cells were then mixed (Figures 5G and 5H). These results characterize SHISA6 as a cell-autonomous Wnt inhibitor.

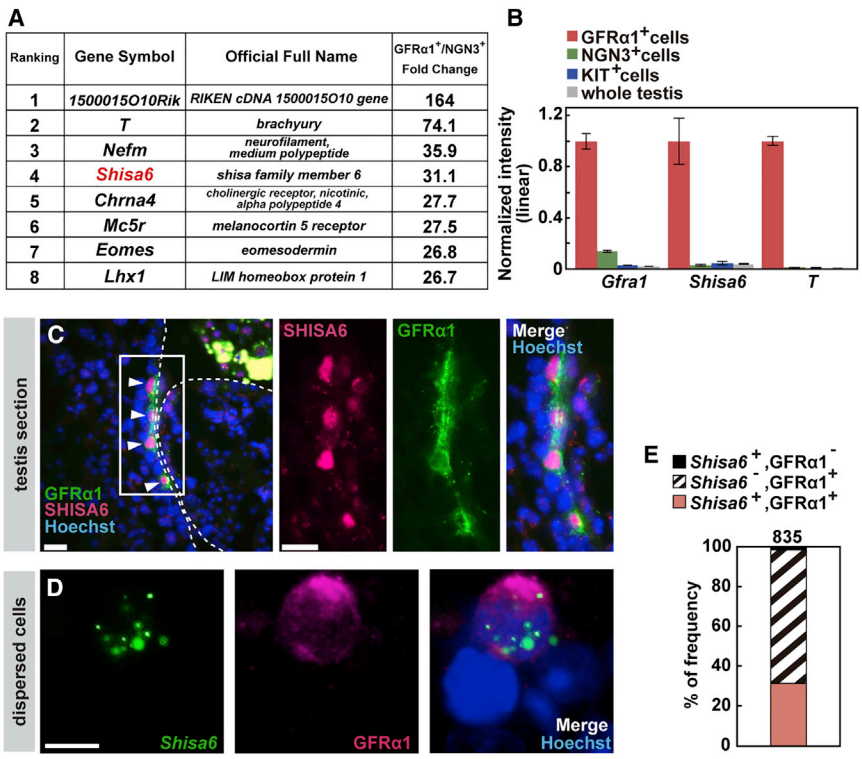

Ranking	Gene Symbol	Official Full Name	GFRα1+/NGN3+ Fold Change
1	*1500015O10Rik*	*RIKEN cDNA 1500015O10 gene*	164
2	*T*	*brachyury*	74.1
3	*Nefm*	*neurofilament, medium polypeptide*	35.9
4	*Shisa6*	*shisa family member 6*	31.1
5	*Chrna4*	*cholinergic receptor, nicotinic, alpha polypeptide 4*	27.7
6	*Mc5r*	*melanocortin 5 receptor*	27.5
7	*Eomes*	*eomesodermin*	26.8
8	*Lhx1*	*LIM homeobox protein 1*	26.7

Figure 4. Expression of *Shsia6* in Mouse Testes

(A) List of genes showing the highest enrichments in the GFRα1+ fraction over the NGN3+ fraction in our microarray analysis.

(B) Expression profiles summarized from the microarray data. Represented as means ± SEM (n = 3 microarrays each form different mice).

(C) IF images of adult wild-type (WT) mice, stained for SHISA6 and GFRα1. Arrowheads and square indicate the SHISA6+ spermatogonia and the magnified areas on the right panel, respectively. Seminiferous tubules are outlined by dashed lines. Scale bar, 20 μm.

(D and E) Representative image (D) and quantification (E) of dissociated testicular cells of adult mice, doubly stained for *Shisa6* by fluorescence in situ hybridization (FISH) and for GFRα1 by IF. A total of 835 cells from five mice were counted. Scale bar, 10 μm.

Although some SHISA proteins inhibit FGF signal (Furushima et al., 2007; Yamamoto et al., 2005), SHISA6 only weakly suppressed the FGF signal in HEK293T cells (Figure 5I). GDNF signal was not inhibited (Figure 5J).

SHISA6 Confers Resistance to Wnt/β-Catenin Signaling to Maintain the GFRα1+ Cell Pool

In common with the GFRα1+ cells, GS cells expressed a high level of SHISA6 in the presence of GDNF (Figures 6A and 6B), allowing us to test the SHISA6 role in vitro. We found that activation of an *Ngn3-luc* reporter by the Wnt/β-catenin pathway (using WNT3a and R-spondin2) was augmented when cells were co-transfected with *Shisa6* small interfering RNA (siRNA) (Figure 6C), supporting the idea that SHISA6 lowers differentiation-promotion by WNT.

Next, we asked whether the SHISA6 function in vivo, by generating *Shisa6*-null alleles using the CRISPR/Cas9 system (Figures 6D, 6E, and S5A–S5D) (Cong et al., 2013), including $Shisa6^{\Delta 6+502}$ (referred to as $Shisa6^{KO}$ hereafter; Figures 6E–6K, S5C–S5K, and S6A–S6D). $Shisa6^{KO/+}$ and $Shisa6^{KO/KO}$ mice grew seemingly healthy with normal body weights (Figure S5F). Unexpectedly, $Shisa6^{KO/KO}$ mice did not show apparent defects in their GFRα1+ cell pool and overall spermatogenesis (Figures S5E and S5G–S5K). However, a compound mutation analysis revealed that *Shisa6* genetically interacts with *β-catenin*. While *fl(ex3)/+* or $Shisa6^{KO/+}$ mice showed a normal GFRα1+ cell pool size (Figures 2K and S5K), $Shisa6^{KO/+}$; *fl(ex3)/+* mice had a significant reduction in the GFRα1+ pool, similar to the *fl(ex3)/fl(ex3)* mice (Figures 6I–6K and S6A–S6D). This was unlikely due to off-target effects, since consistent phenotypes were observed for another *Shisa6* null allele: $Shisa6^{\Delta 1}$ (Figures S6E–S6G).

Shisa6 Is Expressed in *T* (*Brachyury*)-Positive Cells Showing Stem Cell Characters

Finally, we sought to understand the properties of the *Shisa6*+ subset of GFRα1+ cells. Given the limited immunodetectability and genetic tools, we made use of gene(s) that show concordant expression with *Shisa6*, as an alternative strategy. Among genes that similarly showed high enrichments to GFRα1+ fraction (Figure 4A), we focused on *T* (*Brachyury*). Because, an engineered *T* allele ($T^{nEGFP\text{-}CreERT2}$) was available in which nuclear (n)-GFP and CreERT2 (a tamoxifen-inducible Cre) were flanked to the endogenous Brachyury via 2A peptides, and these proteins were simultaneously generated from a single polycistronic mRNA transcribed from the *T* locus (Figure 7A) (Imuta et al., 2013). This enabled reliable visualization and tracing of the T+ cells, using GFP and CreERT2, respectively. In the $T^{nEGFP\text{-}CreERT2/+}$ mouse testes, *Shisa6* expression was specifically detected in a majority (~70%) of *T*-GFP+ cells, which comprised of ~40% of GFRα1+

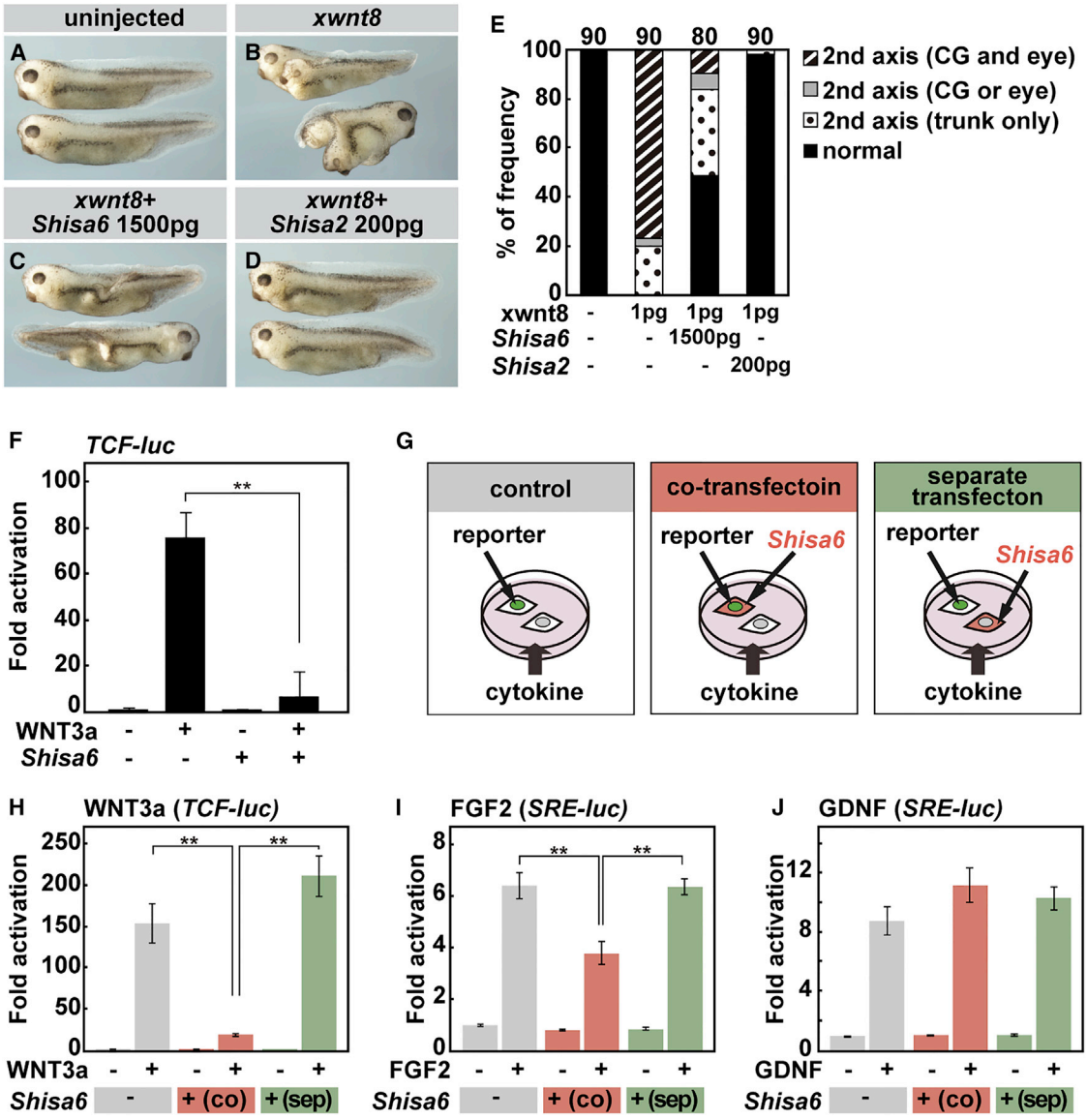

Figure 5. SHISA6 Is a Cell-Intrinsic Wnt Inhibitor

(A–D) Representative appearances of *Xenopus laevis* embryos at stage 33–35, after injection of the indicated combination of mRNAs.

(E) Quantification of data in (A–D), classified by the presence or absence of a duplicated (second) body axis and the degree of anteriorization (e.g., with or without cement gland [CG] and/or eyes). Numbers of counted embryos are shown above.

(F) Effects of SHISA6 on *TCF-luc* activity stimulated by WNT3a. HEK293T cells were transfected with the *TCF-luc* reporter and the *Shisa6*-expression or the empty vector. Twenty-four hours later, cells were stimulated with WNT3a for another 24 hr before analysis (n = 3 independent experiments).

(G–J) Cell-autonomous and non-cell-autonomous effects of SHISA6 on WNT3a, FGF2, and GDNF signaling. HEK293T cells were transfected with a luciferase reporter plasmid (*TCF-luc* or *SRE-luc*) and pcDNA3-*Shisa6* either simultaneously (co-transfection) or separately. Transfected cells were then mixed as schematically shown in (G), followed by stimulation with WNT3a (H), FGF2 (I), or GDNF (J) for 24 hr (n = 3 independent experiments). Luciferase assays were then performed. In (J), expression plasmids for GFRα1 and RET were also co-transfected with *SRE-Luc* reporter to reconstruct a receptor for GDNF.

Represented as means ± SEM. **p < 0.01 (Student's t tests). See also Figure S4.

spermatogonia (Figures 7B–7F). Based on this considerable concordance, properties of T^+ cells were then studied to gain insights into the SHISA6$^+$ cells.

Morphologically, the *T*-GFP$^+$ population was composed of a higher percentage of A_s cells, compared with the T-GFP$^-$/GFRα1$^+$ cells (Figure 7G), and observed throughout

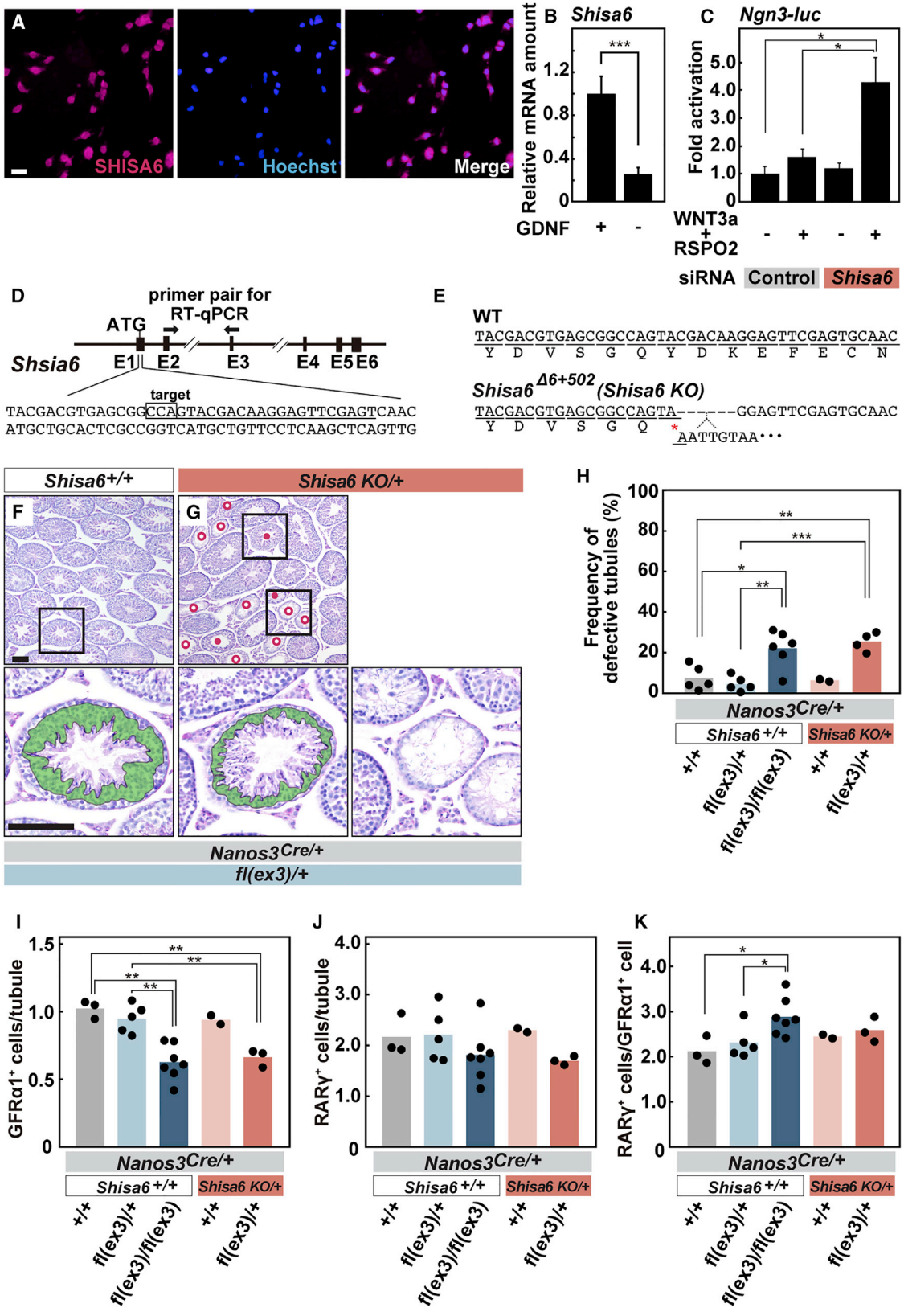

(legend on next page)

the seminiferous epithelial cycle (Figure 7H). The function of T^+ cells in steady-state spermatogenesis was also examined following pulse-labeling by tamoxifen-activation of CreERT2 (Figures 7I–7L). Two days after pulse, a fraction of *T*-GFP$^+$ cells was successfully labeled by a lineage reporter: *R26RH2B*-mCherry (Figure 7J) (Abe et al., 2011). At 1 month, and also at 6 months, the induced cells (labeled with GFP, in this case) formed large patches occupying seminiferous tubule segments, indicating that at least a part of T^+ cells contributed to long-term spermatogenesis (Figures 7K and 7L). These characteristics of T^+ (and probably SHISA6$^+$) cells were relevant to stem cell functions.

DISCUSSION

In this study, we demonstrated that Wnt/β-catenin signaling drove the differentiation of GFRα1$^+$ spermatogonia to NGN3$^+$. This study reinforced and complemented the previous reports that combined in vitro culture with transplantation-based stem cell assays (Yeh et al., 2011, 2012) and that analyzed the in vivo impact of *β-catenin* deletion (Takase and Nusse, 2016). First, because GFRα1$^+$ and NGN3$^+$ cells both form repopulating colonies in the recipient's testes after transplantation (Grisanti et al., 2009; Nakagawa et al., 2007), it was difficult to unambiguously link the results of the transplantation assay with the states of differentiation. This present study directly showed that Wnt/β-catenin signaling upregulates the *Ngn3* expression in vitro (Figure 1F). Second, because *β-catenin* also contributes to cell adhesion and cytoskeletal regulation (Takeichi, 2014), the *β-catenin* deletion study inevitably leaves some ambiguity about the role of Wnt/β-catenin signal. This study showed that stabilization of β-catenin, showing weaker impact on cell adhesion (Harada et al., 1999), reduced the GFRα1$^+$ pool in vivo (Figure 2K). This was in agreement with enhanced differentiation, and largely consistent with the results of *β-catenin* deletion (Figures S3B–S3M; Takase and Nusse, 2016). Wnt/β-catenin signaling inhibits stem cell differentiation In many cases, e.g., interfollicular epidermis, small intestinal crypts, and embryonic stem cells (Kim et al., 2005; Lim et al., 2013; Sato et al., 2004). Mouse spermatogenesis illustrates the less-investigated, differentiation-promotion by WNT, as observed in the melanocyte stem cells during hair follicle regeneration (Rabbani et al., 2011). Takase and Nusse (2016) concluded that Wnt/β-catenin signaling stimulates the proliferation of PLZF$^+$ undifferentiated spermatogonia. We, therefore, examined the proliferation status of GFRα1$^+$ cells in the C*tnnb1* mutants, and found no significant differences, or consistent trends, compared with those in the C*tnnb1*$^{+/+}$ mice (Figure S7A). Therefore, Wnt/β-catenin signaling may stimulate the proliferation of NGN3$^+$ (i.e., PLZF$^+$/GFRα1$^-$) cells, in addition to the GFRα1$^+$-to-NGN3$^+$ differentiation.

We characterized SHISA6 as a Wnt inhibitor that acts in a cell-autonomous manner, which also inhibits FGF signaling to a weaker extent (Figures 5A–5J and S4A–S4E). Interestingly, SHISA6 has been recently reported to desensitize AMPA receptor in the CNS (Klaassen et al., 2016). SHISA6 is, therefore, a context-dependent dual functional protein. In the testes, *Shisa6* expression was restricted to a small subset of GFRα1$^+$ spermatogonia. We generated null alleles of *Shisa6* and found that a decrease in SHISA6 acted cooperatively with the stabilization of β-catenin in the reduction of the GFRα1$^+$ cell pool. Collectively, these observations strongly suggest that SHISA6 plays a role in the maintenance of the GFRα1$^+$ pool by reducing the Wnt/β-catenin signaling strength in the SHISA6$^+$ cells. SHISA6

Figure 6. SHISA6 Confers Resistance to Wnt/β-Catenin Signaling In Vitro and In Vivo

(A) IF image of GS cells stained with an anti-SHISA6 antibody. Scale bar, 20 μm.

(B) *Shisa6* mRNA expression in GS cells cultured for three days with or without GDNF, measured by quantitative real-time PCR. Represented as means ± SEM (n = 3 independent experiments).

(C) GS cells were transfected with an *Ngn3-luc* reporter and a *Shisa6* or control siRNA expression vector and cultured for 3 days in the presence or absence of WNT3a and R-spondin2, before luciferase assay. Represented as means ± SEM (n = 3 independent experiments).

(D) Schematics of the *Shisa6* locus and the location of the CRISPR/Cas9 targeting site.

(E) Structure of the *Shisa6*$^{\Delta 6+502}$ allele (*Shisa6*^{KO}), harboring an in-frame stop codon as a result of a 6-bp deletion and a 502-bp insertion.

(F and G) Histological images of testicular sections of adult mice of the indicated genotypes, stained with PAS-hematoxylin. Lower panels are the magnified images of the indicated regions in the upper panels. Open and closed red dots indicate the tubule sections with lost or exiguous germ cell layer(s) (see the lower panels in which tubule sections at stage I are shown with round spermatid layers colored in green), and those containing Sertoli cells only, see the lower right panel of (G), respectively. Scale bar, 100 μm.

(H) Percentages of total defective tubules (lost or exiguous germ cell layer(s)) in mice with indicated genotypes.

(I–K) Average number of GFRα1$^+$ (I) and RARγ$^+$ (J) cells per tubule, and the ratio between RARγ$^+$ and GFRα1$^+$ cells (K) in testes with the indicated genotypes, based on double IF.

(H), (I), (J), and (K) contain re-used data from Figures 2J–2M, respectively.

Throughout, actual values from different individuals and their averages are shown by dots and columns, respectively. *p < 0.05, **p < 0.01, ***p < 0.001 (Student's t test). See also Figures S5 and S6.

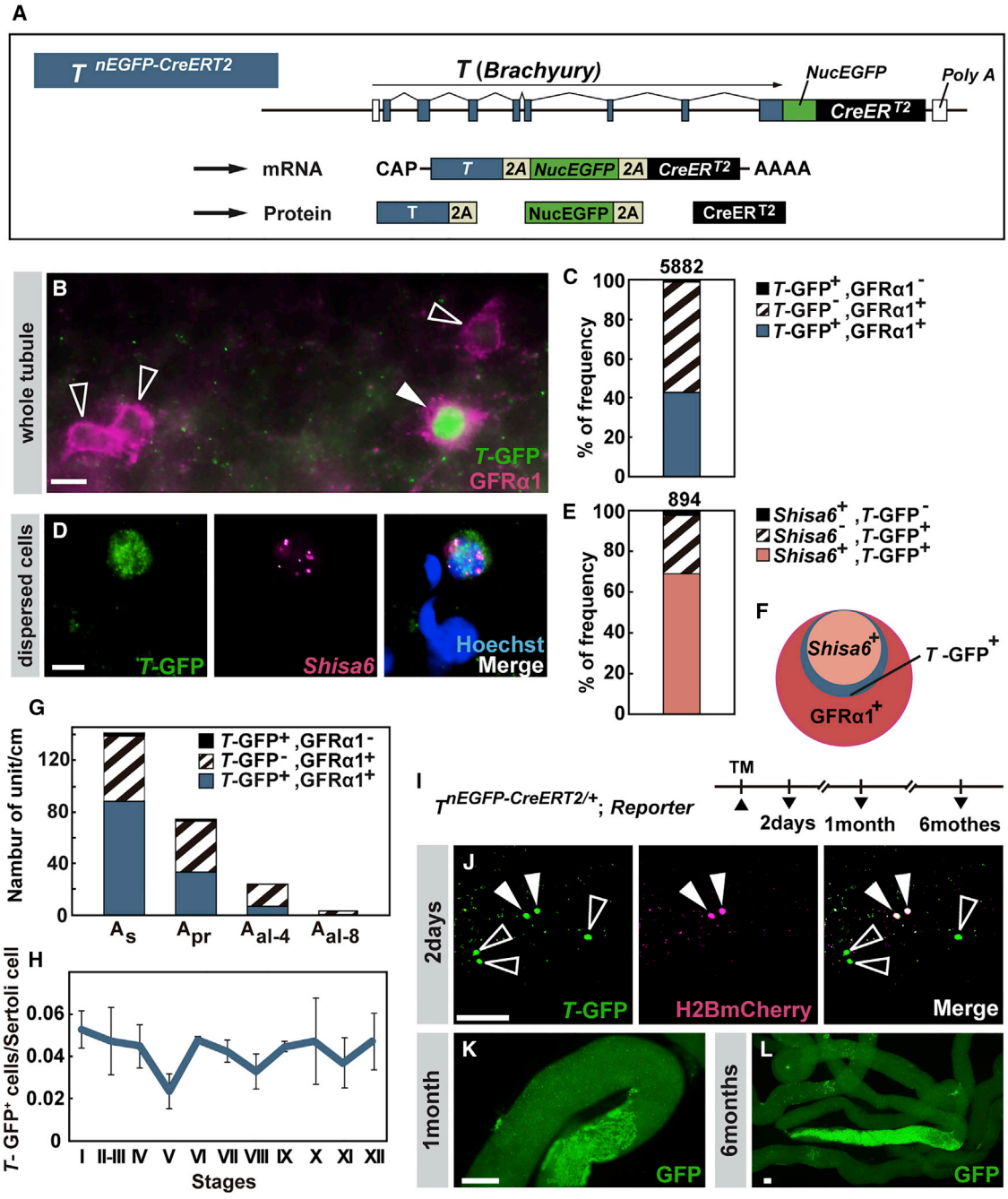

Figure 7. Characterization of the Subset of GFRα1$^+$ Cells Expressing *Shisa6* and *T*

(A) Schematic of the structure of the $T^{nEGFP\text{-}CreERT2}$ allele (Imuta et al., 2013).

(B and C) IF image (B) and quantification (C) of whole-mount IF of seminiferous tubules of $T^{nEGFP\text{-}CreERT2}$ adult mice stained for GFP and GFRα1. Open and filled arrowheads indicate *T*-EGFP$^-$/and *T*-EGFP$^+$/GFRα1$^+$ cells, respectively. A total of 5,882 cells from four mice were counted.

(D and E) Representative image (D) and quantification (E) of dissociated testicular cells of $T^{nEGFP\text{-}CreERT2}$ adult mice doubly stained for *Shisa6* by FISH and for GFP. 894 cells from three mice were counted.

(F) Schematic presentation of the relationship between *Shisa6*$^+$, *T*-GFP$^+$, and GFRα1$^+$ populations, summarized from (C), (E) and Figure 4E. Areas of each circle are proportional to the numbers of these populations, indicating their nested relationship.

(legend continued on next page)

probably achieves this function by affecting the expression of Wnt receptors on the cell surface, conjectured from the function of *xshisa1* (Yamamoto et al., 2005), although other mechanisms are not excluded.

It is puzzling to observe in this study that the stabilizing *β-catenin* mutation, which acts dominantly in many other tissues, affected the GFRα1$^+$ cell pool only when introduced homozygously, and that heterozygous deletion of *β-catenin* caused affected spermatogenesis. These findings imply that Wnt/β-catenin signal is strongly suppressed in stem spermatogonia. *Shisa6* appears to be involved in this suppression; however, a lack of an apparent phenotype in *Shisa6*$^{KO/KO}$ mice suggests that multiple mechanisms are involved. Other cell-autonomous Wnt inhibitor(s) could also be involved, such as *Shisa2*, whose expression was also enriched in the GFRα1$^+$ fraction (Figure S7B). We also speculate that the nuclear accumulation of β-catenin could be prevented by sequestration by E-cadherin, as proposed in the colon epithelium, which also requires homozygous introduction of the stabilizing *β-catenin* mutation to transform (Huels et al., 2015). In accordance with this, undifferentiated spermatogonia express high levels of E-cadherin (Nakagawa et al., 2010; Tokuda et al., 2007), and showed prominent cytoplasmic β-catenin staining in GFRα1$^+$ cells (Figure S7C).

This study illustrates a unique mode of Wnt inhibitor function. Many Wnt inhibitors are secreted proteins, act in a non-cell-autonomous manner, and tune the spatial pattern of Wnt activity. These include Dickkopf proteins (*Dkk*s), secreted Frizzled-related proteins (*Sfrp*s), and Wnt inhibitory factor 1 (*Wif1*). Similarly, cell-autonomous Wnt inhibitors identified so far (*xshisa1*, *xshisa2*, *xshisa3*, *Apcdd1*, *Tiki1*, and *flop1/2*) also shape the spatial patterns of Wnt activity (Cruciat and Niehrs, 2013; Miyagi et al., 2015). In contrast, this study suggests that heterogeneous *Shisa6* expression variegates the stem/progenitor spermatogonia in terms of their sensitivity to Wnt/β-catenin signaling in a spatially uniform facultative microenvironment.

Given that SHISA6 confers resistance to differentiation-inducing Wnt/β-catenin signaling, SHISA6$^+$ cells should be a key population to understand this stem cell system. Although their in-depth characterization was difficult, we could analyze T (Brachyury)$^+$ cells that showed a major overlap with *Shisa6*$^+$ cells, taking advantage of an engineered allele. T$^+$/GFRα1$^+$ cells are morphologically more biased to A$_s$ cells, compared with the T$^-$/GFRα1$^+$ cells (Figure 6E), and persist throughout the cycle of the seminiferous epithelium (Figure 7G). Furthermore, pulse-labeled T$^+$ cells showed a long-term contribution to spermatogenesis (Figures 7G–7L). These features of T$^+$ cells are postulated for the stem cells. Echoing with this is the suggestion that *T* is crucial for the self-renewing potential of cultured spermatogonia (Wu et al., 2011). We assume that *Shisa6*$^+$ cells also showed similar stem cell-related characteristics, although we cannot formally exclude the possibility that only the T$^+$/SHISA6$^-$ cells exhibited the long-term stem cell functions.

It is not easy, however, to be conclusive with the identity of stem cells (Yoshida, 2017). A number of genes (e.g., *Id4*, *Pax7*, *Erbb3*, and *Bmi1*) have been reported to delineate subsets of GFRα1$^+$ cells showing stem cell-related characteristics, like what has been shown for T$^+$ (and probably SHISA6$^+$) cells in this study. Understandably, it is proposed that cells expressing these genes are the bona fide stem cells. It is puzzling, however, that these genes appear to delineate different populations. For example, the observed frequencies were very different, namely, 1.1 ± 0.1 *Id4*-GFP$^+$ cells/tubule section (Chan et al., 2014) and about one PAX7$^+$ cell in an entire testis cross-section (which usually contains >100 tubules) (Aloisio et al., 2014); these genes show very different degrees of enrichment to the GFRα1$^+$ fraction (Figure S7D). Furthermore, intravital live-imaging studies demonstrated that GFRα1$^+$ cells continually interconvert between the states of A$_s$, A$_{pr}$, and A$_{al}$ through incomplete division and intercellular bridge breakdown (Hara et al., 2014). Combined with clonal fate analysis and mathematical modeling, it is proposed that the entire GFRα1$^+$ population may comprise a single stem cell pool. This stem cell system, therefore, should be more complex and dynamic than has been considered, where SHISA6$^+$/T$^+$ cells (or *states*) should play some key roles. A considerable hypothesis is that GFRα1$^+$ cells may interconvert between SHISA6/T-positive and -negative states, which show high and low potentials of self-renewal, respectively.

In conclusion, we propose a generic mechanism underlying the heterogeneous stem cell fates in facultative

(G) Frequency of *T*-GFP$^+$/and *T*-GFP$^-$/GFRα1$^+$ spermatogonial units showing the morphological entities indicated below. Few syncytia consisting of cells other than 2^n cells were omitted. Counts from four mice were summarized.
(H) Frequency of *T*-GFP$^+$ cells along the seminiferous epithelial cycle (n = 3 testes).
(I–L) Pulse labeling and fate analysis of *T*$^+$ spermatogonia. Following the indicated experimental schedule (I), adult mice harboring the *T*$^{nEGFP\text{-}CreERT2}$ allele and a lineage reporter (*R26R-H2B-mCherry* or *CAG-CAT-EGFP*) were injected with 4-hydroxytamoxifen (TM) and killed at different time points. (J) IF image of whole-mount seminiferous tubules two days after TM pulse, stained for *T*-GFP and DsRed. Open and filled arrowheads indicate *T*-GFP$^+$ cells and induced cells, respectively. (K) and (L) IF images of whole-mount seminiferous tubules at 1 month (K) and 6 months (L) after labeling (with GFP). Note the large patches of GFP$^+$ cells.
Scale bars, 10 μm for (B) and (D) and 100 μm for (J) and (K).

niche environments: different levels of cell-autonomous inhibitor (SHISA6, in this case) may confer heterogeneous resistance to uniformly distributed differentiation-promoting extracellular signaling (such as WNTs). Here, stem cells with higher levels of inhibitors would remain in the undifferentiated cell pool with higher probabilities, while those with lower inhibitor levels are more inclined to differentiate.

EXPERIMENTAL PROCEDURES

Animals

Ngn3/EGFP (Yoshida et al., 2006), *Gfra1*^{EGFP} (Enomoto et al., 2000), *Ctnnb1*$^{fl(ex3)}$ (Harada et al., 1999), *Ctnnb1*^{fl} (also designated as *β-catenin*^{flox} or *β-catenin*$^{\Delta ex2-6\text{-}fl}$) (Brault et al., 2001), *Nanos3-Cre* (Suzuki et al., 2008), *Gdnf-LacZ* (Moore et al., 1996), *CAG-CAT-EGFP* (Kawamoto et al., 2000), *R26R-H2B-mCherry* (Abe et al., 2011), and *T*$^{nEGFP\text{-}CreERT2}$ (Imuta et al., 2013) mice were described previously. The *Shisa6 KO* allele was generated as described in the Supplemental Information. All mice were maintained in the C57BL/6 background (Japan CLEA or Charles River Japan). All animal experiments were conducted in accordance with the approval of the Institutional Animal Care and Use Committee of National Institutes of Natural Sciences or as specified.

Cell Culture, Luciferase Assays, and Knockdown Experiments

GS cells derived from the C57BL/6 × ICR intercrossed mice (Araki et al., 2010) were maintained according to Kanatsu-Shinohara et al. (2003), with modifications as described in the Supplemental Information. Transfection was performed using Lipofectamine 2000 (Thermo Fisher Scientific); luciferase assays were performed using a Dual-Luciferase Assay System (Promega). Expression vector for *Shisa6* (pcDNA3-*Shisa6*) was constructed by inserting the *Shisa6* ORF (FANTOM Clone M5C1056A20, Genbank: XM_006533619) into a pcDNA3 vector (Invitrogen). *Shisa6* knockdown was carried out by transfecting cells with Silencer Select pre-designed (non-inventoried) siRNA. Detailed procedures and the vectors used were listed in the Supplemental Information.

Cell Sorting and Microarray Analysis

The GFRα1^{+} fraction was collected from *Gfra1*$^{EGFP/+}$ mice as the GFP^{+} fraction, and the NGN3^{+} and KIT^{+} fractions were collected from *Ngn3/EGFP*$^{Tg/+}$ mice as GFP^{+}/KIT^{-} and GFP^{+}/KIT^{+} fractions, respectively, using an EPICS ALTRA instrument (Beckman Coulter), as described previously (Ikami et al., 2015). The results were partly published previously (Ikami et al., 2015), with the dataset deposited in the GEO (GEO: GSE75532). Additional information was provided in Figure S1 and the Supplemental Information.

Quantitative Real-Time PCR Analyses

Quantitative real-time PCR was performed with a LightCycler 480 System (Roche), using a THUNDEREBIRD SYBR qPCR Mix (Toyobo), after total RNA was reverse-transcribed using a SuperScript III First-Strand Synthesis SuperMix for quantitative real-time PCR primed with a mixture of oligo(dT) and random hexamers (Invitrogen, Life Technologies). Expression of *β-actin* was used for normalization. The primers used were listed in the Supplemental Information.

ISH and IF

ISH was performed as described by Yoshida et al. (2001). Stages of the seminiferous epithelium were determined on adjacent sections, periodic acid-Schiff (PAS) stained using Schiff's reagent (Wako). IF was carried out on cryosectioned 4% paraformaldehyde-fixed, or freshly frozen (for SHISA6), testes. Whole-mount IF for seminiferous tubules was performed as published previously (Nakagawa et al., 2010). For combined fluorescent ISH with IF, ISH was first performed on testicular single-cell suspension using an RNAscope Fluorescent Multiplex Kit (Advanced Cell Diagnostics), followed by IF. The detailed procedures, probes, and antibodies used were described in the Supplemental Information.

Pulse-Chase Experiments

T$^{nEGFP\text{-}CreERT2}$; *R26R-H2B-mCherry* or *T*$^{nEGFP\text{-}CreERT2}$; *CAG-CAT-EGFP* mice were injected intraperitoneally with 2.0 mg of 4-hydroxytamoxifen per individual (Sigma), as reported previously (Hara et al., 2014; Nakagawa et al., 2010). After specific chase periods, the testes were removed and analyzed by IF.

Xenopus laevis Embryo Experiments

Experiments using *Xenopus laevis* embryos were performed as described by Morita et al. (2010). In brief, *xwnt8*, *mShisa6*, *mShisa2* were subcloned into the pSP64T, pCSf107mT, pCSf107mT vectors, respectively, with which capped mRNAs were synthesized using the mMACHINE SP6 Kit (Ambion). mRNAs were injected into the ventral marginal zone of four-cell-stage embryos, as reported previously (Glinka et al., 1997). Injected embryos were incubated in 3% Ficoll/0.1× Steinberg's solution at 13°C overnight, then in 0.3× Marc's modified ringer solution at 13°C for 6 days until reaching stage 33–35.

SUPPLEMENTAL INFORMATION

Supplemental Information includes Supplemental Experimental Procedures and seven figures and can be found with this article online at http://dx.doi.org/10.1016/j.stemcr.2017.01.006.

AUTHOR CONTRIBUTIONS

M.T., S.Y., N.U., and S. Takada designed the research plan; M.T., K.I., Y.K., K.H., and H.M. performed in vivo experiments; M.T., K.I., R.T., T.S., T.O., H.M., and S.Y. performed in vitro experiments; C.N., M.T., and S.K. performed cell sorting and microarray analysis; S.M., F.S., S. Takahashi, and M.M.T. generated gene modified animals; C.T., A.M., N.U., and M.T. performed the experiments using *Xenopus* embryos; M.T. and S.Y. wrote the manuscript.

ACKNOWLEDGMENTS

We are grateful to Y. Saga (*Nanos3*^{Cre}), H. Enomoto (*Gdnf*^{LacZ}), H. Sasaki (*T*$^{nEGFP\text{-}CreERt2}$), T. Fujimori (*R26R-H2B-mCherry*), and J. Miyazaki (*CAG-CAT-EGFP*) for the use of the mice indicated, and to

T. Ishitani for the *TCF-luc* plasmid. We also thank T. Fujimori, M. Tanaka, R. Nishinakamura, and current and former Yoshida lab members for support and discussions, the Model Animal Research Facility (NIBB Bioresource Center) for animal care, and the NIBB Core Research Facilities for support with microarray analyses and the use of an ABI 3130xl sequencer. This work was partly supported in part by Grants-in-Aid for Scientific Research (KAKENHI; 20116004, 24247041, and 25114004 to S.Y., 24111002 to S. Takada, and 25114002 to S.K.).

Received: December 16, 2016
Revised: January 9, 2017
Accepted: January 9, 2017
Published: February 9, 2017

REFERENCES

Abe, T., Kiyonari, H., Shioi, G., Inoue, K., Nakao, K., Aizawa, S., and Fujimori, T. (2011). Establishment of conditional reporter mouse lines at ROSA26 locus for live cell imaging. Genesis *49*, 579–590.

Airaksinen, M.S., and Saarma, M. (2002). The GDNF family: signalling, biological functions and therapeutic value. Nat. Rev. Neurosci. *3*, 383–394.

Aloisio, G.M., Nakada, Y., Saatcioglu, H.D., Pena, C.G., Baker, M.D., Tarnawa, E.D., Mukherjee, J., Manjunath, H., Bugde, A., Sengupta, A.L., et al. (2014). PAX7 expression defines germline stem cells in the adult testis. J. Clin. Invest. *124*, 3929–3944.

Araki, Y., Sato, T., Katagiri, K., Kubota, Y., and Ogawa, T. (2010). Proliferation of mouse spermatogonial stem cells in microdrop culture. Biol. Reprod. *83*, 951–957.

Brault, V., Moore, R., Kutsch, S., Ishibashi, M., Rowitch, D.H., McMahon, A.P., Sommer, L., Boussadia, O., and Kemler, R. (2001). Inactivation of the beta-catenin gene by Wnt1-Cre-mediated deletion results in dramatic brain malformation and failure of craniofacial development. Development *128*, 1253–1264.

Chan, F., Oatley, M.J., Kaucher, A.V., Yang, Q.E., Bieberich, C.J., Shashikant, C.S., and Oatley, J.M. (2014). Functional and molecular features of the Id4+ germline stem cell population in mouse testes. Genes Dev. *28*, 1351–1362.

Chen, C.C., Chen, H.Y., Su, K.Y., Hong, Q.S., Yan, B.S., Chen, C.H., Pan, S.H., Chang, Y.L., Wang, C.J., Hung, P.F., et al. (2014). Shisa3 is associated with prolonged survival through promoting β-catenin degradation in lung cancer. Am. J. Respir. Crit. Care Med. *190*, 433–444.

Chiarini-Garcia, H., Hornick, J.R., Griswold, M.D., and Russell, L.D. (2001). Distribution of type A spermatogonia in the mouse is not random. Biol. Reprod. *65*, 1179–1185.

Chiarini-Garcia, H., Raymer, A.M., and Russell, L.D. (2003). Non-random distribution of spermatogonia in rats: evidence of niches in the seminiferous tubules. Reproduction *126*, 669–680.

Clevers, H., and Nusse, R. (2012). Wnt/beta-catenin signaling and disease. Cell *149*, 1192–1205.

Cong, L., Ran, F.A., Cox, D., Lin, S., Barretto, R., Habib, N., Hsu, P.D., Wu, X., Jiang, W., Marraffini, L.A., et al. (2013). Multiplex genome engineering using CRISPR/Cas systems. Science *339*, 819–823.

Cruciat, C.M., and Niehrs, C. (2013). Secreted and transmembrane wnt inhibitors and activators. Cold Spring Harbor Perspect. Biol. *5*, a015081.

de Rooij, D.G., and Russell, L.D. (2000). All you wanted to know about spermatogonia but were afraid to ask. J. Androl. *21*, 776–798.

Enomoto, H., Heuckeroth, R.O., Golden, J.P., Johnson, E.M., and Milbrandt, J. (2000). Development of cranial parasympathetic ganglia requires sequential actions of GDNF and neurturin. Development *127*, 4877–4889.

Fuller, M.T., and Spradling, A.C. (2007). Male and female Drosophila germline stem cells: two versions of immortality. Science *316*, 402–404.

Furushima, K., Yamamoto, A., Nagano, T., Shibata, M., Miyachi, H., Abe, T., Ohshima, N., Kiyonari, H., and Aizawa, S. (2007). Mouse homologues of Shisa antagonistic to Wnt and Fgf signalings. Dev. Biol. *306*, 480–492.

Gely-Pernot, A., Raverdeau, M., Celebi, C., Dennefeld, C., Feret, B., Klopfenstein, M., Yoshida, S., Ghyselinck, N.B., and Mark, M. (2012). Spermatogonia differentiation requires retinoic acid receptor gamma. Endocrinology *153*, 438–449.

Glinka, A., Wu, W., Onichtchouk, D., Blumenstock, C., and Niehrs, C. (1997). Head induction by simultaneous repression of Bmp and Wnt signalling in Xenopus. Nature *389*, 517–519.

Grasso, M., Fuso, A., Dovere, L., de Rooij, D.G., Stefanini, M., Boitani, C., and Vicini, E. (2012). Distribution of GFRA1-expressing spermatogonia in adult mouse testis. Reproduction *143*, 325–332.

Grisanti, L., Falciatori, I., Grasso, M., Dovere, L., Fera, S., Muciaccia, B., Fuso, A., Berno, V., Boitani, C., Stefanini, M., et al. (2009). Identification of spermatogonial stem cell subsets by morphological analysis and prospective isolation. Stem Cells *27*, 3043–3052.

Hara, K., Nakagawa, T., Enomoto, H., Suzuki, M., Yamamoto, M., Simons, B.D., and Yoshida, S. (2014). Mouse spermatogenic stem cells continually interconvert between equipotent singly isolated and syncytial states. Cell Stem Cell *14*, 658–672.

Harada, N., Tamai, Y., Ishikawa, T., Sauer, B., Takaku, K., Oshima, M., and Taketo, M.M. (1999). Intestinal polyposis in mice with a dominant stable mutation of the beta-catenin gene. EMBO J. *18*, 5931–5942.

Hasegawa, K., and Saga, Y. (2014). FGF8-FGFR1 signaling acts as a niche factor for maintaining undifferentiated spermatogonia in the mouse. Biol. Reprod. *91*, 145.

Hogarth, C.A., Arnold, S., Kent, T., Mitchell, D., Isoherranen, N., and Griswold, M.D. (2015). Processive pulses of retinoic acid propel asynchronous and continuous murine sperm production. Biol. Reprod. *92*, 37.

Hovanes, K., Li, T.W., Munguia, J.E., Truong, T., Milovanovic, T., Lawrence Marsh, J., Holcombe, R.F., and Waterman, M.L. (2001). Beta-catenin-sensitive isoforms of lymphoid enhancer factor-1 are selectively expressed in colon cancer. Nat. Genet. *28*, 53–57.

Huels, D.J., Ridgway, R.A., Radulescu, S., Leushacke, M., Campbell, A.D., Biswas, S., Leedham, S., Serra, S., Chetty, R., Moreaux, G., et al. (2015). E-cadherin can limit the transforming properties of activating β-catenin mutations. EMBO J. *34*, 2321–2333.

Ikami, K., Tokue, M., Sugimoto, R., Noda, C., Kobayashi, S., Hara, K., and Yoshida, S. (2015). Hierarchical differentiation competence

in response to retinoic acid ensures stem cell maintenance during mouse spermatogenesis. Development *142*, 1582–1592.

Imuta, Y., Kiyonari, H., Jang, C.W., Behringer, R.R., and Sasaki, H. (2013). Generation of knock-in mice that express nuclear enhanced green fluorescent protein and tamoxifen-inducible Cre recombinase in the notochord from Foxa2 and T loci. Genesis *51*, 210–218.

Jijiwa, M., Kawai, K., Fukihara, J., Nakamura, A., Hasegawa, M., Suzuki, C., Sato, T., Enomoto, A., Asai, N., Murakumo, Y., et al. (2008). GDNF-mediated signaling via RET tyrosine 1062 is essential for maintenance of spermatogonial stem cells. Genes Cells *13*, 365–374.

Kanatsu-Shinohara, M., Ogonuki, N., Inoue, K., Miki, H., Ogura, A., Toyokuni, S., and Shinohara, T. (2003). Long-term proliferation in culture and germline transmission of mouse male germline stem cells. Biol. Reprod. *69*, 612–616.

Kawamoto, S., Niwa, H., Tashiro, F., Sano, S., Kondoh, G., Takeda, J., Tabayashi, K., and Miyazaki, J. (2000). A novel reporter mouse strain that expresses enhanced green fluorescent protein upon Cre-mediated recombination. FEBS Lett. *470*, 263–268.

Kim, K.A., Kakitani, M., Zhao, J., Oshima, T., Tang, T., Binnerts, M., Liu, Y., Boyle, B., Park, E., Emtage, P., et al. (2005). Mitogenic influence of human R-spondin1 on the intestinal epithelium. Science *309*, 1256–1259.

Klaassen, R.V., Stroeder, J., Coussen, F., Hafner, A.S., Petersen, J.D., Renancio, C., Schmitz, L.J., Normand, E., Lodder, J.C., Rotaru, D.C., et al. (2016). Shisa6 traps AMPA receptors at postsynaptic sites and prevents their desensitization during synaptic activity. Nat. Commun. *7*, 10682.

Klein, A.M., and Simons, B.D. (2011). Universal patterns of stem cell fate in cycling adult tissues. Development *138*, 3103–3111.

Klein, A.M., Nakagawa, T., Ichikawa, R., Yoshida, S., and Simons, B.D. (2010). Mouse germ line stem cells undergo rapid and stochastic turnover. Cell Stem Cell *7*, 214–224.

Kubota, H., Avarbock, M.R., and Brinster, R.L. (2004). Growth factors essential for self-renewal and expansion of mouse spermatogonial stem cells. Proc. Natl. Acad. Sci. USA *101*, 16489–16494.

Lim, X., Tan, S.H., Koh, W.L., Chau, R.M., Yan, K.S., Kuo, C.J., van Amerongen, R., Klein, A.M., and Nusse, R. (2013). Interfollicular epidermal stem cells self-renew via autocrine Wnt signaling. Science *342*, 1226–1230.

Meng, X., Lindahl, M., Hyvonen, M.E., Parvinen, M., de Rooij, D.G., Hess, M.W., Raatikainen-Ahokas, A., Sainio, K., Rauvala, H., Lakso, M., et al. (2000). Regulation of cell fate decision of undifferentiated spermatogonia by GDNF. Science *287*, 1489–1493.

Miyagi, A., Negishi, T., Yamamoto, T.S., and Ueno, N. (2015). G protein-coupled receptors Flop1 and Flop2 inhibit Wnt/beta-catenin signaling and are essential for head formation in Xenopus. Dev. Biol. *407*, 131–144.

Moore, M.W., Klein, R.D., Farinas, I., Sauer, H., Armanini, M., Phillips, H., Reichardt, L.F., Ryan, A.M., Carver-Moore, K., and Rosenthal, A. (1996). Renal and neuronal abnormalities in mice lacking GDNF. Nature *382*, 76–79.

Morita, H., Nandadasa, S., Yamamoto, T.S., Terasaka-Iioka, C., Wylie, C., and Ueno, N. (2010). Nectin-2 and N-cadherin interact through extracellular domains and induce apical accumulation of F-actin in apical constriction of Xenopus neural tube morphogenesis. Development *137*, 1315–1325.

Morrison, S.J., and Spradling, A.C. (2008). Stem cells and niches: mechanisms that promote stem cell maintenance throughout life. Cell *132*, 598–611.

Nagano, T., Takehara, S., Takahashi, M., Aizawa, S., and Yamamoto, A. (2006). Shisa2 promotes the maturation of somitic precursors and transition to the segmental fate in Xenopus embryos. Development *133*, 4643–4654.

Nakagawa, T., Nabeshima, Y., and Yoshida, S. (2007). Functional identification of the actual and potential stem cell compartments in mouse spermatogenesis. Dev. Cell *12*, 195–206.

Nakagawa, T., Sharma, M., Nabeshima, Y., Braun, R.E., and Yoshida, S. (2010). Functional hierarchy and reversibility within the murine spermatogenic stem cell compartment. Science *328*, 62–67.

Rabbani, P., Takeo, M., Chou, W.C., Myung, P., Bosenberg, M., Chin, L., Taketo, M.M., and Ito, M. (2011). Coordinated activation of Wnt in epithelial and melanocyte stem cells initiates pigmented hair regeneration. Cell *145*, 941–955.

Russell, L.D., Ettlin, R.A., Sinha, H.A.P., and Clegg, E.D. (1990). Histological and Histopathological Evaluation of the Testis (Cache River Press).

Sada, A., Hasegawa, K., Pin, P.H., and Saga, Y. (2012). NANOS2 acts downstream of glial cell line-derived neurotrophic factor signaling to suppress differentiation of spermatogonial stem cells. Stem Cells *30*, 280–291.

Sato, N., Meijer, L., Skaltsounis, L., Greengard, P., and Brivanlou, A.H. (2004). Maintenance of pluripotency in human and mouse embryonic stem cells through activation of Wnt signaling by a pharmacological GSK-3-specific inhibitor. Nat. Med. *10*, 55–63.

Shimizu, N., Kawakami, K., and Ishitani, T. (2012). Visualization and exploration of Tcf/Lef function using a highly responsive Wnt/beta-catenin signaling-reporter transgenic zebrafish. Dev. Biol. *370*, 71–85.

Snippert, H.J., van der Flier, L.G., Sato, T., van Es, J.H., van den Born, M., Kroon-Veenboer, C., Barker, N., Klein, A.M., van Rheenen, J., Simons, B.D., et al. (2010). Intestinal crypt homeostasis results from neutral competition between symmetrically dividing Lgr5 stem cells. Cell *143*, 134–144.

Spradling, A., Fuller, M.T., Braun, R.E., and Yoshida, S. (2011). Germline stem cells. Cold Spring Harbor Perspect. Biol. *3*, a002642.

Stine, R.R., and Matunis, E.L. (2013). Stem cell competition: finding balance in the niche. Trends Cell Biol. *23*, 357–364.

Sugimoto, R., Nabeshima, Y., and Yoshida, S. (2012). Retinoic acid metabolism links the periodical differentiation of germ cells with the cycle of Sertoli cells in mouse seminiferous epithelium. Mech. Dev. *128*, 610–624.

Suzuki, H., Tsuda, M., Kiso, M., and Saga, Y. (2008). Nanos3 maintains the germ cell lineage in the mouse by suppressing both Bax-dependent and -independent apoptotic pathways. Dev. Biol. *318*, 133–142.

Takase, H.M., and Nusse, R. (2016). Paracrine Wnt/beta-catenin signaling mediates proliferation of undifferentiated spermatogonia in the adult mouse testis. Proc. Natl. Acad. Sci. USA *113*, E1489–E1497.

Takeichi, M. (2014). Dynamic contacts: rearranging adherens junctions to drive epithelial remodelling. Nat. Rev. Mol. Cell Biol. *15*, 397–410.

Tokuda, M., Kadokawa, Y., Kurahashi, H., and Marunouchi, T. (2007). CDH1 is a specific marker for undifferentiated spermatogonia in mouse testes. Biol. Reprod. *76*, 130–141.

von Engelhardt, J., Mack, V., Sprengel, R., Kavenstock, N., Li, K.W., Stern-Bach, Y., Smit, A.B., Seeburg, P.H., and Monyer, H. (2010). CKAMP44: a brain-specific protein attenuating short-term synaptic plasticity in the dentate gyrus. Science *327*, 1518–1522.

Wu, X., Goodyear, S.M., Tobias, J.W., Avarbock, M.R., and Brinster, R.L. (2011). Spermatogonial stem cell self-renewal requires ETV5-mediated downstream activation of Brachyury in mice. Biol. Reprod. *85*, 1114–1123.

Yamamoto, A., Nagano, T., Takehara, S., Hibi, M., and Aizawa, S. (2005). Shisa promotes head formation through the inhibition of receptor protein maturation for the caudalizing factors, Wnt and FGF. Cell *120*, 223–235.

Yeh, J.R., Zhang, X., and Nagano, M.C. (2011). Wnt5a is a cell-extrinsic factor that supports self-renewal of mouse spermatogonial stem cells. J. Cell Sci *124*, 2357–2366.

Yeh, J.R., Zhang, X., and Nagano, M.C. (2012). Indirect effects of Wnt3a/beta-catenin signalling support mouse spermatogonial stem cells in vitro. PLoS One *7*, e40002.

Yoshida, S. (2012). Elucidating the identity and behavior of spermatogenic stem cells in the mouse testis. Reproduction *144*, 293–302.

Yoshida, S., Ohbo, K., Takakura, A., Takebayashi, H., Okada, T., Abe, K., and Nabeshima, Y. (2001). Sgn1, a basic helix-loop-helix transcription factor delineates the salivary gland duct cell lineage in mice. Dev. Biol. *240*, 517–530.

Yoshida, S., Takakura, A., Ohbo, K., Abe, K., Wakabayashi, J., Yamamoto, M., Suda, T., and Nabeshima, Y. (2004). Neurogenin3 delineates the earliest stages of spermatogenesis in the mouse testis. Dev. Biol. *269*, 447–458.

Yoshida, S., Sukeno, M., Nakagawa, T., Ohbo, K., Nagamatsu, G., Suda, T., and Nabeshima, Y. (2006). The first round of mouse spermatogenesis is a distinctive program that lacks the self-renewing spermatogonia stage. Development *133*, 1495–1505.

Yoshida, S., Sukeno, M., and Nabeshima, Y. (2007). A vasculature-associated niche for undifferentiated spermatogonia in the mouse testis. Science *317*, 1722–1726.

Yoshida, Y. (2017). Regulatory mechanism of spermatogenic stem cells in mice: their dynamic and context-dependent behavior. In Reproductive & Developmental Strategies,, K. Kobayashi, T. Kitano, Y. Iwao, and M. Kondo, eds. (Springer), Chapter 12.